

Targeted Delivery System Based on Magnetic Mesoporous Silica Nanocomposites with Light-Controlled Release Character

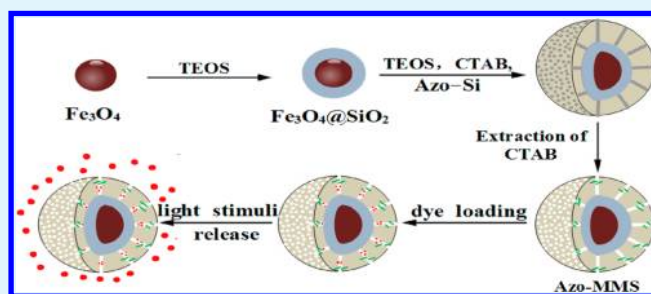
Yanyan Wang,^{†,‡} Bin Li,^{*,†} Liming Zhang,[†] Hang Song,^{*,†} and Ligong Zhang[†]

[†]State Key Laboratory of Luminescence and Applications, Changchun Institute of Optics Fine Mechanics and Physics, Chinese Academy of Sciences, Changchun 130033, P. R. China

[‡]Graduate School of the Chinese Academy of Sciences, Chinese Academy of Sciences, Beijing 100039, P. R. China

S Supporting Information

ABSTRACT: We report the facile synthesis and easy operation of a smart delivery system based on core–shell structured magnetic mesoporous silica nanocomposites covalently grafted with light-responsive azobenzene derivatives, which integrates magnetic targeting and stimuli-responsive release property. Irradiation with visible light triggers the release of guest molecules loaded in the mesopores.



KEYWORDS: magnetic, mesoporous silica, core–shell, targeting, light-responsive, drug delivery

In the development of efficient and safe drug delivery systems that provide therapeutic levels of drugs in specific organs, tissues, or even cellular structures, where and when required has received much attention in recent years.¹ The release mechanism of many conventional biodegradable delivery systems relies on hydrolysis-induced erosion of carrier structure, so the release of these matrix-encapsulated compounds usually takes place immediately upon dispersion of these composites in water.² However, the delivery of many toxic antitumor drugs requires “zero release” before reaching target cells or tissues. Therefore, it is highly desirable to design delivery systems that can be activated by stimuli to control the release of guest molecules and stable enough under physiological conditions. To achieve this goal, we consider the delivery system to consist of both a stimuli-responsive component and an appropriate container.

The use of stimuli-responsive component offers an interesting opportunity for delivery system to become an active participant, rather than passive vehicle. Recently, controlled release delivery systems have been reported responding to a range of stimuli, including light, pH, competitive binding, enzymes, redox activation and so on.³ For therapeutic applications, light is preferable as an external and noninvasive method of actuation. Such a release mode is advantageously independent of the conditions of biological environment, enabling a precise and explicit of release. Many light-sensitive molecules have been used to construct light-responsive systems.⁴ Among them, azobenzene derivatives are very attractive because of their easy trans/cis isomerization, and particularly they can be operated in aqueous environments. For example, they have been utilized as useful photoactivated gatekeepers in pure mesoporous silica materials.⁵ However,

pure mesoporous silica-based devices are difficult to simultaneously achieve targeting and controlled release because of their limited functions, which compromises their practical application in drug delivery systems. In addition to the controlled release of drugs, the targeted delivery is also vitally important to reduce toxic side effects of drugs and enhance drug efficacy.

As a family of novel functional nanomaterials, magnetic nanocomposites with ordered mesoporous silica structures are very useful containers for molecules because of their unique features such as stable mesoporous structure, large surface area, tunable pore size and volume for hosting molecules with various sizes, shape, functionality, and especially well-defined magnetic property that is very desirable for site-specific delivery.⁶ It is believed that the combination of magnetic mesoporous silica nanocomposites with stimuli-responsive component in a single nanovehicle can potentially construct a delivery system with the ability to control the location, time, and amount of drug released. Recently, Zhao and co-workers have explored biomedical applications of ligand exchange triggered drug delivery system based on magnetic mesoporous microspheres capped with nanoparticles.⁷ Despite these achievements, as far as we know, core–shell magnetic mesoporous silica nanocomposites with light-responsive character for controlled-release targeted delivery system have rarely been reported.

Herein, we report azobenzene-modified core–shell magnetic mesoporous silica nanocomposites that can be used as a

Received: October 29, 2012

Accepted: December 17, 2012

Published: December 17, 2012

Scheme 1. Fabrication Strategy and Controlled-Release Procedure of the Targeted Delivery System

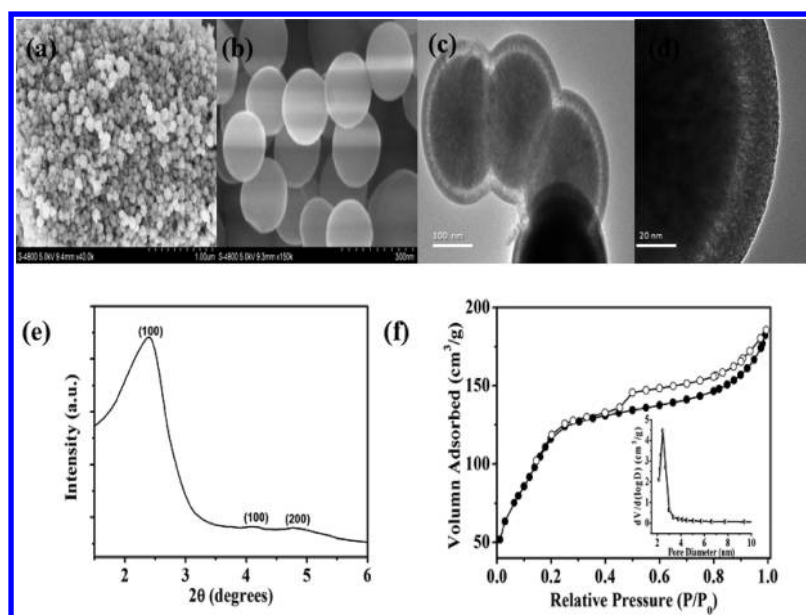
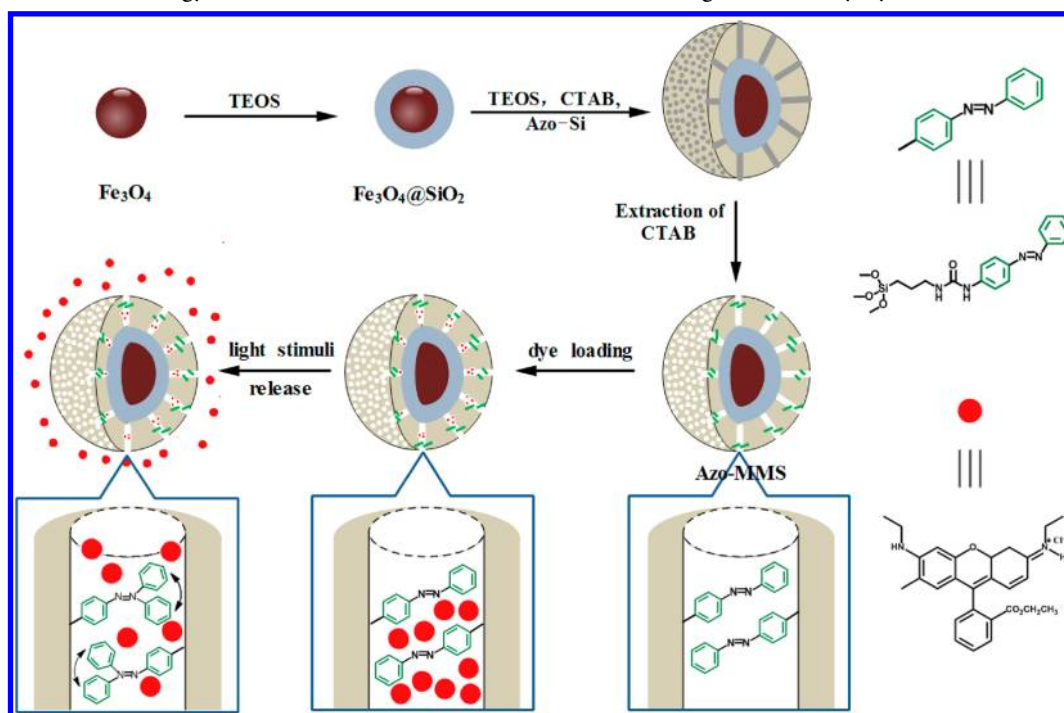


Figure 1. SEM image of (a) Fe_3O_4 and (b) Azo-MMS, TEM images of (c) Azo-MMS and (d) its magnified view, (e) the low-angle XRD pattern of the Azo-MMS, and (f) nitrogen adsorption–desorption isotherms and (inset) pore size distribution of Azo-MMS.

photocontrolled release targeted system for guest molecule. The fabrication and controlled-release procedures of the delivery system are shown in Scheme 1. The as-prepared magnetic Fe_3O_4 nanoparticles were treated by a modified Stöber procedure to prepare the nonporous silica coated Fe_3O_4 (denoted as $\text{Fe}_3\text{O}_4@\text{nSiO}_2$). Subsequently, 4-phenylazoaniline covalently grafted to 3-(triethoxysilyl)propyl isocyanate (denoted as Azo-Si) was used as the sol–gel precursor, TEOS was used as silica source, and cetyltrimethylammonium bromide (CTAB) was selected as the organic template for the formation of the outer mesoporous silica layer.⁸ Finally, the template was removed by solvent extraction to realize the formation of

azobenzene-functionalized core–shell magnetic mesoporous silica nanocomposites (denoted as Azo-MMS). FT-IR analysis (see the Supporting Information, Figure S1) shows the as-synthesized and surfactant-extracted Azo-MMS, indicating that the template has been successfully removed and Azo group in the Si–O–Si framework remains intact after both the hydrolysis–condensation reaction and surfactant extraction. This synthetic procedure is fast, simple and low cost. As for the wide-angle XRD patterns (see the Supporting Information, Figure S2), the Azo-MMS microspheres have similar diffraction peaks to those of the parent Fe_3O_4 particles, proving the well-retained magnetite phase in silica matrix. Compared with the

magnetite particles (Figure 1a), the obtained Azo-MMS (Figure 1b) exhibits a more regular spherical shape, because of smooth surface with mean diameter of ~ 200 nm due to the deposition and growth of silica by the sol–gel process.⁹ A typical core–shell structure with magnetic Fe_3O_4 particle as the core and two distinct silica layers as the outer shell is clearly shown by the transmission electron microscopy (TEM) images (Figure 1c). The mesochannels on the shell are perpendicular to the microsphere surface (Figure 1d), which favors the adsorption and release of guest molecules. Furthermore, the low-angle XRD pattern and N_2 adsorption/desorption isotherms confirm the presence of ordered hexagonal mesopores (Figure 1d and e). The Brunauer–Emmett–Teller (BET) surface area, average pore size, and total pore volume are calculated to be $446 \text{ m}^2 \text{ g}^{-1}$, 2.4 nm, and $0.26 \text{ cm}^3 \text{ g}^{-1}$, respectively.

To evaluate the controlled release performance of Azo-MMS system, we chose rhodamine 6G as the guest molecule. The mechanism of controlled release is based on the photoisomerization of azobenzene derivatives.¹⁰ Azobenzene exists in two configurations (trans and cis), and both the cis and trans derivative conformers absorb light at 450 nm, which causes isomerization and results in a dynamic wagging of the moving parts of the azobenzene derivative.¹¹ As illustrated in scheme 1, when Azo-MMS is exposed to light activation, rhodamine 6G molecules will be released. Prior to the excitation, the guest molecules hosted in the pores cannot diffuse out because of the blocking by high density azobenzene chains. Excitation causes a dynamic wagging motion of azobenzene chains, opening diffusion pathways and expelling the guest molecules out of the pores. To perform this study, we carried out the delivery operation in the presence and absence of light actuation (450 nm). Detailed experimental process is given in the Supporting Information. As shown in the Figure 2, the relative fluorescence

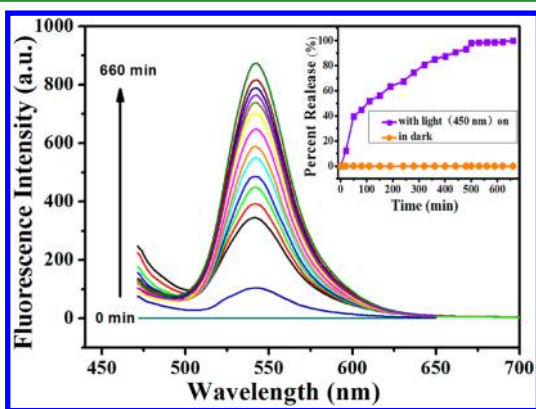


Figure 2. Emission spectra of cargo release when the Azo-MMS nanoparticles were continuously exposed to the light actuation (450 nm). The inset shows the data with and without continuous light actuation as a release profile.

intensity of the solution increases as the Azo-MMS microspheres are continuously exposed to light, suggesting that the rhodamine 6G molecules have been released by light actuation. From the release profile depicted in Figure 2 inset, we can find that when no light activation is used, the unactivated azobenzene chains are able to keep guest molecules constrained all the time, and no release of guest molecules occurs. To eliminate the possible excitation effect from the activation beam used to excite rhodamine 6G, we irradiated Azo-MMS microspheres with equal power at the wavelength at which

rhodamine 6G adsorbs but azobenzene does not absorb to verify that azobenzene excitation drives the release. It is then found that the excitation beam (460 nm) triggers no release (see the Supporting Information, Figure S3). This result demonstrates that the system only responds to excitation wavelengths that can drive the large amplitude azobenzene motion. If the dynamic motion responsible for controlling release can be turned on and off, it will enable the system to externally start and stop the explosion of dye molecules from the mesopores at will. Figure 3 shows the release profile of dyes

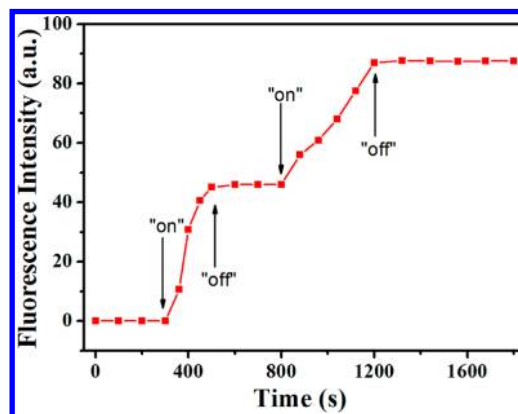


Figure 3. Luminescence intensity-based release plot for the response subjected to periodically switching between 450 nm excitation (“on”) and dark (“off”).

when the excitation of dye-loaded Azo-MMS is periodically turned on and off. We can observe that the particles hold the guest molecules adequately in the dark. The dyes are released from the particles only upon excitation of the Azo-MMS, suggesting that remote control of the release could be achieved.

In addition to the stimuli-response-controlled release property, we demonstrated that Azo-MMS could be led to any specific site of interest by applying external magnetic field. Two cuvettes were charged with rhodamine 6G-loaded Azo-MMS in aqueous solutions. Both cuvettes were held against magnets. As illustrated in panels a and b in Figure 4, the dispersed nanoparticles in both two cuvettes are attracted to the walls of the cuvettes closest to the magnets. Azo-MMS shows no magnetic hysteresis at room-temperature with saturation magnetization value of 39.8 emu g^{-1} , indicating its superparamagnetic character (see the Supporting Information, Figure S4). To demonstrate that the Azo-MMS carrier system could be magnetically directed to a target site where the controlled release is intended to take place, one of the two cuvettes (right) is exposed to light for the release experiment, whereas the other (left) serves as a reference. After 12 h (Figure 4c, d), the solution of the right cuvettes changes to pale pink and exhibits green fluorescence whereas no color and fluorescence can be observed from the contrast solution. This result indicates that dyes are indeed released from Azo-MMS at the targeted location by the introduction of light trigger.

Moreover, one fundamental but crucial question that remains whether this kind of delivery system is suitable for the real drug molecule. For this consideration, we demonstrate this approach using ibuprofen (IBU), which has been widely studied for sustained and controlled drug delivery as a model drug. We monitored the absorbance of the supernatants when the delivery system with and without continuously irradiated at 450 nm. The absorption spectra and the corresponding drug release

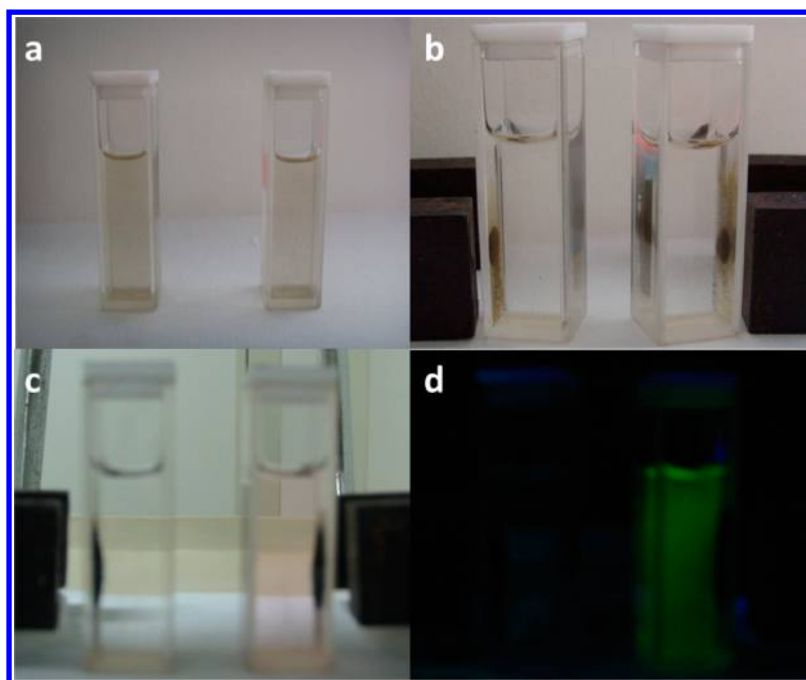


Figure 4. Two cuvettes containing rhodamine 6G-loaded Azo-MMS dispersed in aqueous solutions. Photographs were taken (a) without and (b) with an external magnetic field. With the external magnetic field, the right cuvette was activated by 450 nm, and the photographs were taken (b) before and (c, d) 12 h after the light actuation (c) without and (d) with UV irradiation.

profiles versus release time are depicted as the Figure S5 in the Supporting Information, exhibiting the similar controlled release property as the rhodamine 6G-loaded MMS-Azo does. This result reveals that this system is promising as a candidate of drug carriers. Further work is underway in our laboratory to investigate the cytotoxicity and endocytosis of such nano-system, as well as to test the long-term biocompatibility in vitro and in vivo.

In summary, we reported a smart targeted carrier that was simply prepared by covalently grafting azobenzene derivatives onto the core-shell magnetic mesoporous silica nanocomposites. We have demonstrated that this carrier is effective in releasing cargos upon exposure to light actuation (450 nm), and enables remotely controlled release of the cargo molecules “on-off” at will. Additionally, we have shown the feasibility of using this system as a targeted delivery system by external magnetic field. This composite was also applied to the loading and controlled release of ibuprofen (IBU), demonstrating its potential for applications in drug delivery.

■ ASSOCIATED CONTENT

Supporting Information

Experimental details, FT-IR spectra, XRD pattern, magnetic hysteresis loops and the IBU release curves including cumulative drug release profiles. This material is available free of charge via the Internet at <http://pubs.acs.org>.

■ AUTHOR INFORMATION

Corresponding Author

*E-mail: lib020@yahoo.cn (B.L.).

Notes

The authors declare no competing financial interest.

■ ACKNOWLEDGMENTS

The authors gratefully thank the financial supports of the NSFC (Grants 51172224 and 51103145) and the Science and Technology Developing Project of Jilin Province (Grants 20100533 and 201201009).

■ REFERENCES

- (1) (a) Calderera-Moore, M. E.; Liechty, W. B.; Peppas, N. A. *Acc. Chem. Res.* **2011**, *44*, 1061–1070. (b) Feng, X.; Lv, F.; Liu, L.; Tang, H.; Xing, C.; Yang, Q.; Wang, S. *ACS Appl. Mater. Interfaces* **2010**, *2*, 2429–2435. (c) Fong, W.-K.; Hanley, T.; Boyd, B. J. *J. Controlled Release* **2009**, *135*, 218–226. (d) Rozhkova, E. A. *Adv. Mater.* **2011**, *23*, H136–H150. (e) Xu, Z.; Wang, D.; Guan, M.; Liu, X.; Yang, Y.; Wei, D.; Zhao, C.; Zhang, H. *ACS Appl. Mater. Interfaces* **2012**, *4*, 3424–3431.
- (2) Slowing, I. I.; Trewyn, B. G.; Giri, S.; Lin, V. S. Y. *Adv. Funct. Mater.* **2007**, *17*, 1225–1236.
- (3) (a) Knezevic, N. Z.; Trewyn, B. G.; Lin, V. S. Y. *Chem. Commun.* **2011**, *47*, 2817–2819. (b) Luo, G.-F.; Xu, X.-D.; Zhang, J.; Yang, J.; Gong, Y.-H.; Lei, Q.; Jia, H.-Z.; Li, C.; Zhuo, R.-X.; Zhang, X.-Z. *ACS Appl. Mater. Interfaces* **2012**, *4*, 5317–5324. (c) Leung, K. C. F.; Nguyen, T. D.; Stoddart, J. F.; Zink, J. I. *Chem. Mater.* **2006**, *18*, 5919–5928. (d) Bernardos, A.; Aznar, E.; Marcos, M. D.; Martínez-Mañez, R.; Sancenón, F.; Soto, J.; Barat, J. M.; Amorós, P. *Angew. Chem.* **2009**, *121*, 5998–6001. (e) Zhao, Y.-L.; Li, Z.; Kabehie, S.; Bottros, Y. Y.; Stoddart, J. F.; Zink, J. I. *J. Am. Chem. Soc.* **2010**, *132*, 13016–13025. (f) Croissant, J.; Zink, J. I. *J. Am. Chem. Soc.* **2012**, *134*, 7628–7631. (g) Manna, U.; Patil, S. *ACS Appl. Mater. Interfaces* **2010**, *2*, 1521–1527.
- (4) (a) Alvarez-Lorenzo, C.; Bromberg, L.; Concheiro, A. *Photochem. Photobiol.* **2009**, *85*, 848–860. (b) Johansson, E.; Choi, E.; Angelos, S.; Liang, M.; Zink, J. I. *J. Sol-Gel Sci. Technol.* **2008**, *46*, 313–322.
- (5) (a) Wang, X.; Yang, Y.; Yang, Z.; Liao, Y.; Zhang, W.; Xie, X. *Chin. Sci. Bull.* **2010**, *55*, 3441–3447. (b) Yuan, Q.; Zhang, Y.; Chen, T.; Lu, D.; Zhao, Z.; Zhang, X.; Li, Z.; Yan, C.-H.; Tan, W. *ACS Nano* **2012**, *6*, 6337–6344. (c) Lu, J.; Choi, E.; Tamanoi, F.; Zink, J. I. *Small* **2008**, *4*, 421–426.

- (6) (a) Liu, J.; Qiao, S. Z.; Hu, Q. H.; Lu, G. Q. *Small* **2011**, *7*, 425–443. (b) Deng, Y.; Cai, Y.; Sun, Z.; Zhao, D. *Chem. Phys. Lett.* **2011**, *510*, 1–13.
- (7) Teng, Z.; Zhu, X.; Zheng, G.; Zhang, F.; Deng, Y.; Xiu, L.; Li, W.; Yang, Q.; Zhao, D. *J. Mater. Chem.* **2012**, *22*, 17677–17684.
- (8) (a) Lei, B.; Li, B.; Zhang, H.; Lu, S.; Zheng, Z.; Li, W.; Wang, Y. *Adv. Funct. Mater.* **2006**, *16*, 1883–1891. (b) Deng, Y. H.; Qi, D. W.; Deng, C. H.; Zhang, X. M.; Zhao, D. Y. *J. Am. Chem. Soc.* **2007**, *130*, 28–29. (c) Wang, Y. Y.; Li, B.; Zhang, L. M.; Li, P.; Wang, L. L.; Zhang, J. *Langmuir* **2011**, *28*, 1657–1662.
- (9) Stöber, W.; Fink, A.; Bohn, E. *J. Colloid Interface Sci.* **1968**, *26*, 62–69.
- (10) Tanaka, T.; Ogino, H.; Iwamoto, M. *Langmuir* **2007**, *23*, 11417–11420.
- (11) (a) Sierocki, P.; Maas, H.; Dragut, P.; Richardt, G.; Vögtle, F.; De Cola, L.; Brouwer, F.; Zink, J. I. *J. Phys. Chem. B* **2006**, *110*, 24390–24398. (b) Angelos, S.; Choi, E.; Vögtle, F.; De Cola, L.; Zink, J. I. *J. Phys. Chem. C* **2007**, *111*, 6589–6592.